Pure dephasing in the linear and nonlinear optical response of quantum dots

V M Axt, B Krummheuer, A Vagov and T Kuhn

Institut für Festkörpertheorie, Westfälische Wilhelms-Universität Münster, Wilhelm-Klemm-Str. 10, D-48149, Münster, Germany

Abstract. A comprehensive analysis of the effect of pure dephasing processes on the linear as well as the nonlinear optical response of quantum dots is presented. The focus is on small dots where it is permissible to consider only the lowest energy states. It turns out that pure dephasing can be studied analytically in this limit. The analysis is based on exact closed form expressions for the linear susceptibility as well as for the nonlinear response to a sequence of delta pulses. The dependences of linear absorption spectra on statically applied fields and on the temperature for different dot sizes are discussed. Exact results are compared with calculations based on the correlation expansion. Four-Wave-Mixing spectra are presented for different temperatures and strength of the inhomogeneous broadening. Good qualitative agreement with experiments is found.

1. Introduction

In systems like quantum dots where carriers can only occupy discrete energy levels real phonon emission or absorption processes which do conserve the single particle energies are rather unlikely. This phenomenon is known as *phonon bottleneck* [1]. The coupling to phonons is, however, still a major source for the decoherence of the optical polarization. Here, the parts of the electron-phonon coupling that do not change the electronic occupation numbers play a crucial role. Their contribution is customarily called *pure dephasing* and it is known to be of particular importance in small quantum dots and at elevated temperatures [2, 3, 4, 5]. For many applications of quantum dots as parts of optoelectronic devices [6] a good knowledge of the dephasing is required. This is particularly true if semiconductor quantum dots should be used as basic building blocks for quantum information processing [7, 8, 9] where the operation crucially relies on the presence of coherence.

In the present paper we study the impact of pure dephasing on the linear and non-linear response of small quantum dots. Our analysis is devoted to a situation where the separation of electronic energies is large enough such that a selective excitation is possible even with pulses that are short on the time scale of relevant phonon periods. In this case we can focus on the two electronic states that are resonantly coupled by the optical laser field. After the energy selection has been accounted for by concentrating on only two electronic levels we can exploit that our pulses are assumed to be short compared with the remaining relevant time scales set by the phonon energies and go over to the limit of delta pulses. For this limit we shall present general solutions of our dynamical equations that are non-perturbative with respect to both the coupling to phonons and to the laser light. From our general formulas we calculate linear and four-wave-mixing (FWM) spectra and discuss influences of various quantities such as temperature, dot size and applied static fields. In order to demonstrate the role of multi-phonon contributions we also compare our results with calculations based on the first order correlation expansion which accounts only for single phonon processes.

2. Definition of the model

The starting point for our analysis is the following Hamiltonian of a two level model coupled to phonons and laser light

$$H = \hbar\Omega c^\dagger c - \left(MEc^\dagger d^\dagger + M^*E^*dc\right) + \sum_\xi \hbar\omega_\xi b_\xi^\dagger b_\xi + \sum_\xi \hbar\left[\left(g_\xi^e b_\xi + g_\xi^{e*} b_\xi^\dagger\right) c^\dagger c - \left(g_\xi^h b_\xi + g_\xi^{h*} b_\xi^\dagger\right) d^\dagger d\right], \quad (1)$$

where c, d, b_ξ are the destruction operators for electrons, holes, and phonons, respectively, and $c^\dagger, d^\dagger, b_\xi^\dagger$ are the corresponding creation operators. $g_\xi^{e,h}$ are phonon coupling constants, where the index $\xi = (j, \mathbf{q})$ comprises a phonon wave vector $\mathbf{q}$ and a branch index $j = LO, LA, TA$ for longitudinal optical (LO) or acoustic (LA) phonons or transverse acoustic (TA) modes, respectively. M is the component of the dipole matrix element in direction of the laser field polarization and $E(t)$ stands for the amplitude of the laser field. Finally, Ω is the energy of an electron occupying a conduction band dot state. We have chosen the energy of the hole to define the zero of energy.

While the general formulas that shall be presented in the next section are valid for arbitrary electron and hole wave functions as well as arbitrary phonon dispersions or dependences of the carrier phonon coupling on the phonon modes for a specific evaluation of these formulas these quantities have, of course, to be specified. The numerical results of this paper have been obtained by considering a confinement potential for electron and holes given by an infinite barrier in the z (vertical) direction and a parabolic potential in the x,y (lateral) plane. We use standard GaAs parameters (explicitly given e.g. in Ref. [5]). The same potential shape is taken for electrons and holes, resulting with GaAs parameters in a lateral extension of the hole wave function which is by a factor of $(m_e/m_h)^{(1/4)} \approx 0.87$ smaller than the electron wave function. The vertical size of the dot is given by the well width while we defined the lateral size as the radius where the electron density is reduced to half its maximum value. We shall consider here only the case of equal lateral and vertical sizes.

Concerning the phonon modes we consider a situation where the lattice properties of the dot are not significantly different from the environment such that the phonons can be described as bulk phonons. For bulk phonons the carrier-phonon couplings $g_\xi^{e(h)}$ can be written in the form

$$g_\xi^{e(h)} = \Psi^{e(h)}(\mathbf{q}) G_\xi^{e(h)} \qquad \text{with} \qquad \Psi^{e(h)}(\mathbf{q}) = \int_V \left|\psi_{e(h)}(\mathbf{r})\right|^2 e^{i\mathbf{r}\mathbf{q}} d^3\mathbf{r}, \quad (2)$$

where the form factor $\Psi^{e(h)}(\mathbf{q})$ has been expressed in terms of the wave functions $\psi_{e(h)}(\mathbf{r})$ and $G_\xi^{e(h)}$ is the bulk coupling matrix element. We consider three different types of carrier-phonon coupling: the polar optical coupling to LO phonons, deformation potential coupling to LA phonons, and the piezo-electric coupling to LA and TA phonons. For the corresponding bulk coupling matrix elements standard literature expressions have been taken [10, 5].

The dispersion of the phonon branches is modeled by taking the shape of the dispersion relation of the standard diatomic linear chain model adjusted to the GaAs phonon dispersion relation reported in the literature [11]. Isotropic phonon dispersions have been assumed for all branches. The phonon dispersions obtained in this way are shown in Fig. 1 together with the angular integrated effective form factors

$$\Psi_{eff}(q) := \int_0^{2\pi} d\varphi \int_0^{\pi} d\theta \, \sin(\theta) \, |\Psi_{\mathbf{q}}^e - \Psi_{\mathbf{q}}^h|^2 \quad (3)$$

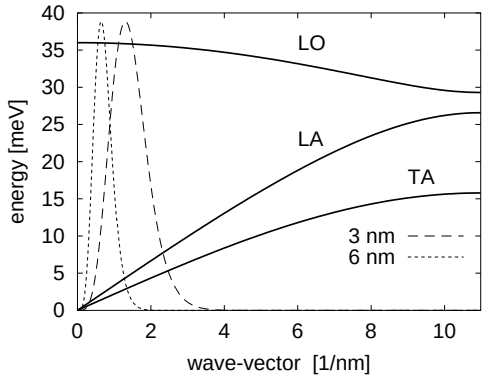

Figure 1. Dispersion relations of the LO, LA, and TA phonons and normalized effective form factors [see Eq. (3)].

that correspond to different dot sizes. This effective form factor directly determines the region in the phonon **q**-space to which the dot is effectively coupled by the polar interaction mechanisms. For the deformation potential coupling a somewhat different quantity should appear in the integral because electrons and holes couple to LA phonons by different deformation potentials. Nevertheless, Eq. (3) provides a good estimate of the range of relevant q-values also in this case. The general tendency is that the form factors extend to higher **q**-values with decreasing sizes of the dots. From Fig. 1 it is seen that even for dot sizes of about 3 nm the deviations from a constant LO phonon frequency only start to become noticeable. Acoustic phonons provide a continuum of energies. Down to the smallest dots studied here Fig. 1 shows that the dispersion of both longitudinal and transverse acoustic phonons is essentially linear. For acoustic phonons the increased relevant range of phonon frequencies with decreasing dot size leads to an effectively increasing width of the coupled continuum.

3. Exact results for the dynamics of generating functions

A convenient way to represent the dynamics of the system is to follow the time evolution of generating functions for phonon assisted density matrices which are defined as

$$Y(\alpha_\xi,t) = \left\langle d\ c\ e^{-\sum_\xi \alpha_\xi^* b_\xi^\dagger} e^{\sum_\xi \alpha_\xi b_\xi} \right\rangle,$$

$$C(\alpha_\xi,t) = \left\langle c^\dagger c\ e^{-\sum_\xi \alpha_\xi^* b_\xi^\dagger} e^{\sum_\xi \alpha_\xi b_\xi} \right\rangle,$$

$$F(\alpha_\xi,t) = \left\langle e^{-\sum_\xi \alpha_{*\xi} b_\xi^\dagger} e^{\sum_\xi \alpha_\xi b_\xi} \right\rangle.$$

For each phonon mode we have introduced a complex valued parameter α_ξ and the brackets denote the quantum mechanical ensemble averaging over electronic and phononic degrees of freedom. These generating functions provide a complete description of the system in the sense that all elements of the electronic and phononic density matrix including all possible electronic and phononic correlation functions can be obtained from Y, C, F. For example, the optical polarization P which is most important for optical experiments can be expressed

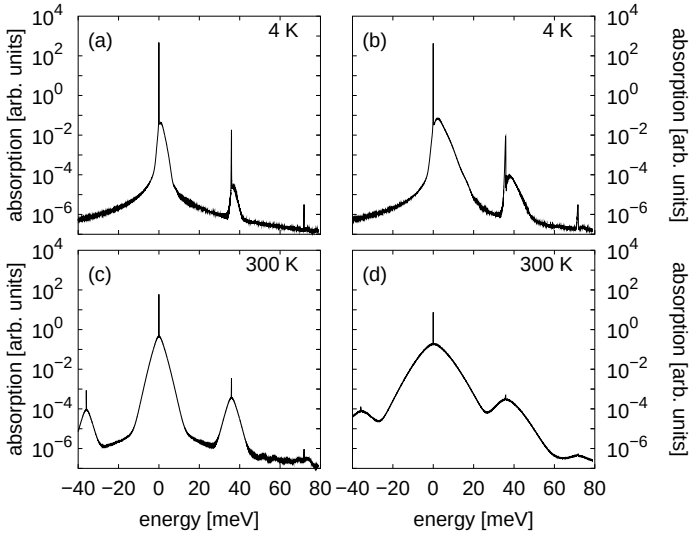

Figure 2. Linear absorption spectra for a 6 nm (left) and a 3 nm (right) quantum dot at different temperatures.

directly in terms of the transition density Y in the form

$$P(t) = M^* Y(\alpha_\xi, t)|_{\alpha_\xi = 0}\,. \tag{4}$$

Similarly, the occupation of the upper dot level $\langle c^\dagger c\rangle$ is given by the values of $C(\alpha_\xi, t)$ at $\alpha_\xi = 0$.

The equations of motion for the generating functions Y, C, F follow directly from the Heisenberg equations for the corresponding operators and have been derived explicitely without invoking any further approximations in Ref. [12]. The most important feature of these equations is that they form a closed set of equations of motion which is an exact and complete representation of the dynamics of our model. Therefore, formulating the dynamics in terms of generating functions avoids the hierarchy problem which is usually encountered when the dynamics is represented in terms of phonon assisted density matrices which are coupled in an infinite hierarchy of equations.

To complete the definition of the dynamical problem one has to specify initial conditions. Here, we shall assume that before the arrival of any light pulse the dot is in its electronic ground state and that the phonon system is in thermal equilibrium at temperature T. This provides for the following initial conditions for the above defined generating functions

$$Y = 0, \qquad C = 0, \qquad F = e^{-\sum_\xi |\alpha_\xi|^2 N_\xi}\,, \tag{5}$$

where $N_\xi = \left[\exp\left(\frac{\hbar\omega_\xi}{k_B T}\right) - 1\right]^{-1}$ is the thermal distribution of the phonons at temperature T.

In Ref. [12] exact solutions of the coupled equations for Y, C and F have been constructed for an excitation with an arbitrary sequence of delta pulses. Especially compact is the result for a single pulse of the form $\frac{\mathbf{ME}}{\hbar} = \frac{A}{2} e^{i\varphi}\,\delta(t)$, where A denotes the pulse area and φ is a phase. In this case the solutions read

$$\begin{aligned} Y(\alpha_\xi, t) &= \frac{i\theta(t)}{2}\sin(A) \\ &\times \exp\Big(-i\overline{\Omega}t + i\varphi + \sum_\xi [\gamma_\xi^*(\alpha_\xi + \gamma_\xi)(e^{-i\omega_\xi t} - 1) - N_\xi |(\alpha_\xi + \gamma_\xi)e^{-i\omega_\xi t} - \gamma_\xi|^2]\Big) \end{aligned} \tag{6}$$

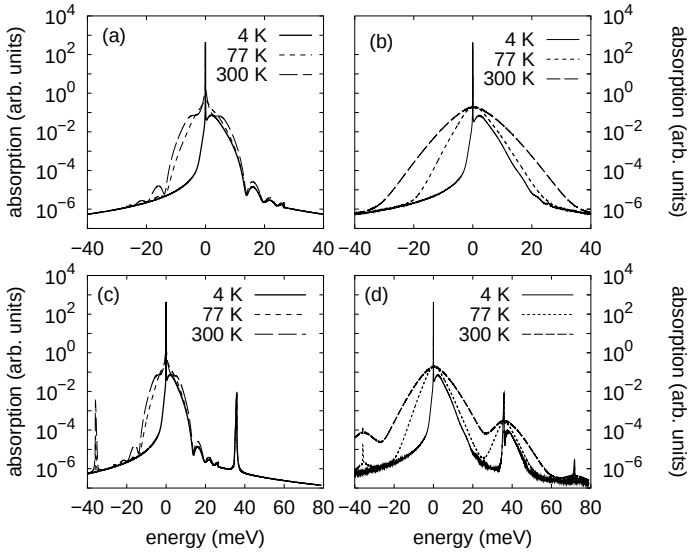

Figure 3. Linear absorption spectra for a 3 nm quantum dot: correlation expansion accounting only for single phonon processes (left), exact results (right). The upper parts are obtained keeping only the deformation potential coupling to LA phonons while all couplings to all phonon modes are accounted for in the lower parts.

$$C(\alpha_\xi,t)=\theta(t)\sin^2(\frac{A}{2})\exp\Big(\sum_\xi 2i\mathrm{Im}\left[\gamma_\xi^*\alpha_\xi\left(e^{-i\omega_\xi t}-1\right)\right]-N_\xi|\alpha_\xi|^2\Big) \tag{7}$$

$$F(\alpha_\xi,t)=\exp\Big(-\sum_\xi N_\xi|\alpha_\xi|^2\Big)\Big\{1+\theta(t)\sin^2(\frac{A}{2})\Big[\exp\Big(2i\mathrm{Im}\Big[\sum_\xi\gamma_\xi^*\alpha_\xi(e^{-i\omega_\xi t}-1)\Big]\Big)-1\Big]\Big\} \tag{8}$$

with $\gamma_\xi=\frac{g_\xi^e-g_\xi^h}{\omega_\xi}$ and $\overline{\Omega}=\Omega-\sum_\xi\left|\gamma_\xi\right|^2\omega_\xi$. Clearly seen is the oscillatory dependence of all components as a function of the pulse area A, which is a manifestation of the Rabi oscillation phenomenon.

4. Linear response

In this section we shall investigated the linear response of our model. A particular focus will be the discussion of linear spectra. Due to their definition, linear spectra are proportional to the imaginary part of the Fourier transform of the polarization induced by a delta pulse. Thus, using delta pulse excitations in our calculations does not limit the results of the present section. Furthermore, the spectra are easily obtained by using Eqs. (4) and (6). In numerically performing the Fourier transform some care has to be taken, because the polarization does not decay to zero for $t\to\infty$ (see e.g. [5]). Thus, before taking the Fourier transform we have muliplied the polarization with a factor e^{-t/t_0} with $t_0=500$ ps. This procedure may be interpreted as a phenomenological way to account for the radiative lifetime.

In Fig. 2 linear spectra are plotted for two different dot sizes [6 nm (left), 3 nm (right)] and two different temperatures [4 K (top), 300 K (bottom)]. The spectrum consist in all cases of a narrow zero phonon line broadend only by the radiative lifetime superimposed on a broad non-Lorentzian background provided by acoustic phonons. This pattern is repeated at the positions of the LO phonon sidebands. Recent FWM measurements revealed that the

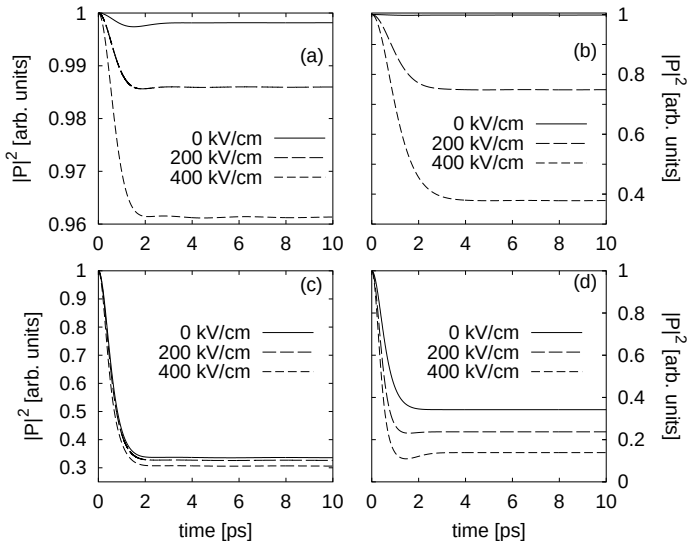

Figure 4. Optical polarizations induced by a δ-pulse for a 6 nm quantum dot interacting with phonons via piezo-electric (a),(b), and deformation potential (c),(d) interaction in the presence of a static vertical (left) and lateral (right) electric field at a temperature of 77 K.

limit of radiative broadening of the zero phonon line is indeed experimentally accessible at low temperatures [13]; at elevated temperatures the zero phonon line exhibits an additional broadening which is not accounted for by the pure dephasing processes covered in our model. Nevertheless, the temperature dependence of the width of the broad backgound is in good agreement with measurements. With rising temperature the strength of the contribution of the zero phonon line clearly decreases relative to the background such that at room temperature the spectra are dominated by the effects of pure dephasing. It is also seen that the lineshapes develop from a strongly asymmetric shape at low temperatures into a highly symmetric form at room temperature, which, however, is still not well represented by a Lorentzian. Finally, the spectra of the 3 nm dot are significantly broader than those of the 6 nm dot, because due to the changes on the form factors a wider part of the continuum is effectively coupled in the former case (see Fig. 3).

In order to clarify the role of multi-phonon processes we have performed calculations using the first order correlation expansion [14]. On this level of theory one accounts for single phonon processes while multi-phonon contributions are neglected. The so obtained approximate spectra are compared with exact results in Fig. 3. The upper parts of the figure show results where only the deformation potential has been accounted for, while in the lower parts all contributions have been included. It is obvious from the figure that the correlation expansion reproduces the width of the full calculation only at low temperatures; at elevated temperatures multi-phonon processes are important and contribute significantly to the broadening. Furthermore, it is seen that the approximate spectra exhibit sharp structures which are absent in the exact result. These structures correspond to energies where a linear absorption with the assistence of only a single phonon is suppresed by unfavorable form factors. The full theory does not show these features, because multi-phonon contributions compensate the suppression. Interestingly, the approximate calculation yields a LO phonon sideband without a broad background. This can be understood from the fact that one LO phonon is needed to produce the sideband and the backgound is then produced by additional acoustic phonon couplings. It is therefore a multi-phonon effect where a LO phonon and further acoustic phonons are involved.

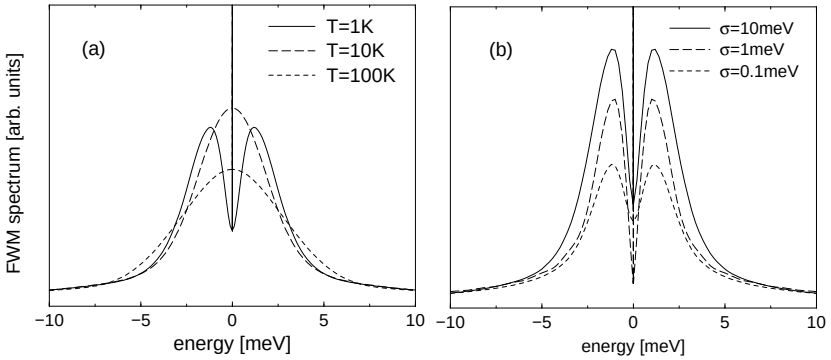

Figure 5. FWM spectra as defined in the text for infinitely strong inhomogeneous broadening at different temperatures (left) and for different width σ of the inhomogegeous broadening (right).

Fig. 4 displays the linear polarization after a delta pulse excitation as a function of time for different additional static fields, which can be applied either vertically (left) or laterally (right). The upper parts are obtained by retaining only the piezo-electric coupling while in the lower parts only the deformation potential coupling has been accounted for. The general trend is that a stronger decoherence is observed for stronger fields. The effect is less pronounced for vertical fields, because here the charge separation induced by the field is limited by the infinite barriers at the boundaries of the dot. The most interesting aspect is, however, that the piezo-electric coupling which is negligible at low fields may become a decoherence mechanism comparable with the deformation potential coupling when strong fields are applied.

5. Nonlinear spectra

From the general results obtained in Ref. [12] it is easy to derive various nonlinear signals. Here, we shall present results on FWM spectra. We consider a two-pulse FWM setup where a first pulse arives at $t=-\tau$ while a second pulse hits the dot at $t=0$. The FWM signal corresponds to the polarization component proportional to $e^{i(2\varphi_2-\varphi_1)}$ where φ_1,φ_2 are the phases of the two pulses. Denoting the respective pulse areas by A_1 and A_2 the FWM signal of a single dot is given by

$$P_{FWM}(t,\tau)=\frac{-iM^*\theta(t)\theta(\tau)}{2}\sin^2(\frac{A_2}{2})\sin(A_1)$$
$$\times e^{i[2\varphi_2-\varphi_1-\bar{\Omega}(t-\tau)]+\sum_\xi|\gamma_\xi|^2[2\cos(\omega_\xi t)-3+e^{i\omega_\xi\tau}(2-e^{i\omega_\xi t})-N_\xi|e^{i\omega_\xi\tau}(2-e^{i\omega_\xi t})-1|^2]}. \quad (9)$$

Recently, corresponding measurements have been performed on an ensemble of dots by using a heterodyne detection technique [13] where the measured signal is proportional to $P_{FWM}(t,\tau)$ averaged over the ensemble. FWM spectra have been extracted in Ref. [13] by taking the time integral of the absolute value of this quantity and performing the Fourier transform with respect to the delay time. Corresponding spectra derived from Eq. (9) are shown in Fig. 5. The left part of the figure displays curves for different temperatures calculated with infinitely strong inhomogenoeous broadening. The spectral shapes for 10 and 100 K are nearly Gaussian and agree qualitatively well with the corresponding measurments Ref. [13]. At extremely low temperatures of the order of ~ 1 K our theory predicts a dip in the lineshape. The lowest temperature for which spectra are reported in Ref. [13] was 50 K. Thus, it is not yet decided whether this can be measured or whether it is suppressed by other mechanisms.

The right part of Fig. 5 shows spectra at 1 K for different values of the width of the inhomogeneous broadening of the ensemble. Interestingly, the dip is more pronounced for stronger inhomogeneous broadening.

6. Conclusions

We have analysed the linear and non-linear response of strongly confined quantum dots by using a generating function approach. Our theory allows for exact solutions for delta pulse excitations. The results are non-perturbative with respect to phonon and light couplings. The spectra obtained in this way exhibit characteristic lineshapes which deviate strongly from a Lorentzian form. Typical spectra consist of a sharp zero phonon line superimposed on a broad background due to acoustic phonons. Lateral or vertical electric fields primarily affect the polar interaction mechanisms which are more efficient due to the separation of charges in static fields. In particular, the piezo-electric coupling may become a relevant decoherence mechanism at high fields. The deformation potential interaction is only weakly influenced by static fields. By comparing exact spectra with results accounting only for single phonon processes we have identified the role of multi-phonon contributions. At elevated temperatures multi-phonon effects are found to contribute significantly to the broadening of the spectra.

In addition we have presented an analysis of FWM spectra. We have shown that inhomogeneous broadening can affect the form of these spectra particularly at low temperatures. Similar to the linear case also the FWM spectra consist of a broad background supplemented by a sharp line. The resulting FWM spectra are in good agreement with corresponding experiments[13].

Acknowledgment. This work has been supported by the European Commission within the Future and Emerging Technologies (FET) project IST-1999-11311 (*Semiconductor-based Implementation of Quantum Information Devices*).

References

[1] Benisty H 1995 Phys. Rev. B 51 13281
[2] Takagahara T 1999 Phys. Rev. B 60 2638
[3] Besombes L, Kheng K, Marsal L and Mariette H 2001 Phys. Rev. B 63 155307
[4] Goupalov S V, Suris R A, Lavallard P and Citrin D S 2001 Nanotechnology 12 518
[5] Krummheuer B, Axt V M and Kuhn T 2002 Phys. Rev. B 65 195313
[6] Bimberg D, Grundmann M. and Ledentsov N N 1998 Quantum dot heterostructures (Chichester: John Wiley and Sons)
[7] Imamoglu A, Awschalom D D, Burkard G, DiVincenzo D P, Loss D, Sherwin M and Small A 1999 Phys. Rev. Lett. 83 4204
[8] Biolatti E, Iotti R C, Zanardi P and Rossi F 2000 Phys. Rev. Lett. 85 5647
[9] Troiani F, Hohenester U and Molinari E 2000 Phys. Rev. B 62 R2263
[10] Mahan G D 1990 Many-Particle Physics, 2nd edn. (New York: Plenum Press)
[11] Adachi S 1994 GaAs and Related Materials (Singapore: World Scientific)
[12] Vagov A, Axt V M and Kuhn T 2002 Phys. Rev. B to be published
[13] Borri P, Langbein W, Schneider S, Woggon U, Sellin R L,Ouyang D and Bimberg D 2001 Phys. Rev. Lett. 87 157401
[14] Kuhn T IN: Theory of Transport Properties of Semiconductor Nanostructures ed by Schöll E 1998 (LONDON Chapman & Hall) p 173